Crystalline Structure of Poly(hexamethylene adipate). Study on the Morphology and the Enzymatic Degradation of Single Crystals

Sebastià Gestí, Ahmed Almontassir, María Teresa Casas, and Jordi Puiggalí*

Departament d'Enginyeria Química, Universitat Politècnica de Catalunya, Avenida Diagonal 647, E-08028, Barcelona, Spain

Received November 10, 2005; Revised Manuscript Received January 9, 2006

The crystalline structure of polyester 6 6 was studied by means of X-ray and electron diffraction and real-space electron microscopy. An orthorhombic unit cell containing eight chain segments with a quasi planar zigzag conformation was derived. The chain axis projection could be defined by a small rectangular cell containing only two molecular segments. Simulation of electron diffraction patterns indicates that molecular segments were arranged with azimuthal angles close to ±46°. X-ray diffraction patterns suggested that the large dimensions of the unit cell were a consequence of a slight shift between neighboring chains that improved the electrostatic interactions. Chain-folded lamellar crystals were obtained by isothermal crystallization of dilute *n*-hexanol or *n*-octanol solutions. The crystalline habit was studied, and the influence of temperature was evaluated. A regular folding surface was observed by using polyethylene decoration techniques. Lamellar crystals were easily degraded with different lipases. A preferential enzymatic attack was, in some cases, observed to occur in the crystal edges, giving rise to highly irregular borders with a fringed texture.

Introduction

Aliphatic polyesters constitute the main group of biodegradable polymers, with their interest being enhanced because of their applications in the biomedical field. The use of glycolide, lactide, and ϵ-caprolactone derivatives as bioabsorbable surgical sutures[1−3] and as polymer matrixes for drug delivery[4] is well-known. Poly(β-hydroxyalkanoate)s synthesized from microorganisms have also received great attention,[5−7] with the optically active polymer of (*R*)-3-hydroxybutyrate (P(3HB)) and its copolymer with (*R*)-3-hydroxyvalerate (P(3HB-*co*-3HV)) probably being the most relevant ones.[8]

Poly(alkylene dicarboxylate)s have lower applications because of the moderate molecular weight that can usually be attained in the thermal polycondensation reaction between diols and dicarboxylic derivatives and to their relatively low melting point. Thus, only five compositions, in which oxalic or succinic acid is used as a dicarboxylic unit, have a melting point higher than 100 °C.[9] The use of diisocyanates as chain extenders allows the final molecular weight to be increased. Some polymers based on poly(butylene succinate)[10] (e.g., Bionolle developed by Showa Highpolymer) are now being commercialized.

Studies on the crystalline structure of aliphatic polyesters and the enzymatic degradation of lamellar single crystals are nowadays receiving considerable attention to achieve a better understanding of the mechanism involved in enzymatic degradation processes. These investigations mainly concern poly(3-hydroxybutyrate),[11−13] poly(lactic acid),[14] and poly(ethylene succinate)[15,16] single crystals. In all cases, crystals are mainly attacked from the crystal edges, rather than from the fold surfaces. This mode of degradation implies a systematic reduction in the crystal size from the edge toward the crystal center. Exo and endo enzymes could participate in this process, but, in contrast, degradation at the chain folds relies on an endo-chain scission.

The determination of the crystalline structure is a basic point to make progress in the study of a degradation mechanism. However, the structure of poly(alkylene dicarboxylate)s has not been extensively studied, probably because of their limited properties. Our recent investigations have aimed to gain insight into this group of polymers, and new packing features have so far been detected.

In general, these polyesters adopt a quasi all-trans conformation when the methylene content of both diol and dicarboxylic units is high.[17,18] However, kink conformations based on a pair of gauche bonds with opposite signs have also been proposed for some ethylene glycol, succinic and adipic acid derivatives.[19−21] Poly(alkylene dicarboxylate)s pack according to monoclinic and orthorhombic unit cells that contain two or four molecular segments.[21,22] The down chain axis projection of the reported structures containing two chain segments corresponds to rectangular unit cells with parameters in the range of $a = 0.500-0.504$ nm, and $b = 0.73-0.75$ nm, although the *a* parameter is doubled for large cells. Nevertheless, recent data obtained with some 1,4-butanediol[23] and 1,6-hexanediol[24] derivatives (polyesters 4 8, 4 10, 4 12, 6 8, and 6 12, whose digits refer to the number of carbon atoms in the diol and the dicarboxylic units) pointed to orthorhombic cells that contain four chain segments and where surprisingly the *b* parameter is doubled. Poly(tetramethylene adipate) deserves a special mention since a streaking of layer lines was observed in the fiber pattern of the crystalline structure associated to an all-trans conformation. This feature suggested a disorder along the chain axis.[25]

The main goal of this paper is to continue with the characterization of polyesters derived from 1,6-hexanediol, and, in particular, to study the crystal morphology and enzymatic degradation of the polymer derived from adipic acid (polyester 6 6). An orthorhombic unit cell with parameters $a = 1.008$ nm, $b = 0.732$ nm, and $c = 1.683$ nm was previously reported by Aylwin and Boyd.[26] A feature of this polymer is the presence of continuous streaks on the layer lines of fiber patterns of unannealed samples, as has been reported for other poly(alkylene

10.1021/bm050860d CCC: $33.50
Published on Web 02/11/2006

dicarboxylate)s. However, in this case, well-defined reflections could be detected on the different layer lines after annealing.

Experimental Section

Polyester 6 6 was synthesized from adipic acid using an excess of 1,4-hexanediol (molar ratio 2.2/1) by thermal polycondensation at 160 °C in a nitrogen atmosphere for 3 h and then in a vacuum at 200 °C for 20 h. Titanium tetrabutoxyde was used as a catalyst. The polymer was dissolved in chloroform and precipitated with ethyl ether. The polymerization yield was 70%. An intrinsic viscosity of 0.8 dL/g was measured with a Cannon-Ubbelhode microviscometer in dichloroacetic acid solutions at 25 ± 0.1 °C. In addition, the molecular weight distribution was determined by size exclusion chromatography (SEC) using a liquid chromatograph (Shimadzu, model LC-8A) equipped with an Empower computer program (Waters). Average molecular weights were calculated using poly(methyl methacrylate) standards. A PL HFIPgel column (Polymer Lab) and a refractive index detector (Shimadzu RID-10A) were used. The polymer was dissolved and eluted in hexafluoroisopropanol at a flow rate of 0.5 mL/min (injected volume, 100 μL; sample concentration, 1.5 mg/mL). Values of 14 400, 25 500, and 1.8 were determined for M_n, M_w, and the polydispersity index, respectively.

Basic calorimetric data was obtained with a Perkin-Elmer DSC−PYRIS 1, using indium metal for calibration. Heating runs were performed at 20 °C/min and a melting temperature of 58 °C was found. The fusion temperature of polyester 6 6 is in agreement with previously reported data (56 °C[26]).

Isothermal crystallizations were carried out in the 0−40 °C range from dilute solutions (0.003% w/v) in alcohols such as *n*-hexanol, *n*-heptanol, and *n*-octanol. A drop of the solution was placed on a carbon-coated grid, and the solvent was allowed to evaporate to avoid a crystal breakage that could be produced when very thin crystals were separated by centrifugation. The crystals were finally shadowed with Pt−carbon at an angle of 15° for bright-field observations. Polymer decoration was achieved by evaporating polyethylene onto the surface of single crystals, as described by Wittmann and Lotz.[27]

A Philips TECNAI 10 electron microscope was used and operated at 80 and 100 kV for bright-field and electron diffraction modes, respectively. Bright-field micrographs were taken with an SIS Mega-View II digital camera. Selected area electron diffraction patterns were recorded on Kodak Tri-X films. The patterns were internally calibrated with gold ($d_{111} = 0.235$ nm). Electron diffraction patterns were digitized, and the intensity of the reflections was determined by means of the ELD program.[28] This also allowed the intensity of saturated reflections to be estimated by a shape-fitting procedure. If a reflection is saturated, the central part of the spot is useless. However, its tail will not be saturated, and so it can be compared to the tail of a Gaussian-type function. A curve-fitting algorithm is used by the program to estimate what the reflection intensity would be if the spot were not saturated.

Degradation of polyester 6 6 single crystals was performed with lipases from *Rhizopus arrhizus* (1500 units/mg) and *Pseudomona cepacia* (40 units/mg). Lamellar crystals, obtained by crystallization in *n*-hexanol at 30 or 40 °C, were deposited on carbon-coated grids. These grids were immersed in 150 μL of a pH 7.0 buffered medium of 50 mM Tris-HCl containing the enzyme (0.03 mg/mL) at a constant temperature of 37 °C. After different exposure times the grids were repeatedly washed with distilled water and ethanol, and finally shadowed with Pt−carbon. Controls without enzyme were also run.

Suspensions of lamellar crystals in the buffered medium (0.5 mg/mL) were incubated at 37 °C with the *Pseudomona cepacia* enzyme (0.03 mg/mL). After the determined exposure times, the crystals were separated by centrifugation and repeatedly washed with distilled water and ethanol. The molecular weights of the exposed samples were determined by gel permeation chromatography (GPC), as explained above.

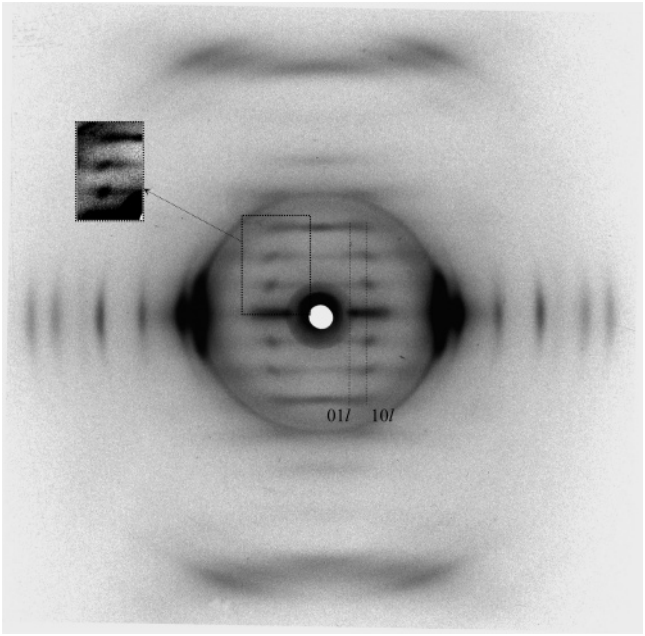

Figure 1. X-ray fiber diffraction pattern of polyester 6 6. Low intensity 01*l* reflections can be seen in the highly exposed pattern shown in the inset.

Atomic force microscope (AFM) examination of single crystals was performed with a Digital Instruments Nanoscope IV under tapping mode using silicon tips with a resonance frequency of 25 kHz and a spring constant of 0.4 N/m. Both height and phase images were recorded simultaneously.

X-ray diagrams were recorded under vacuum at room temperature using calcite as a calibration standard. A modified Statton camera (W. R. Warhus, Wilmington, DE) with Ni−copper radiation of wavelength 0.1542 nm was used. Fibers were prepared from the melt and annealed under stress at 45 °C.

The experimental fiber density was calculated by the flotation method using ethanol and carbon tetrachloride as solvents. A value of 1.14 g/mL was obtained.

Patterns were also recorded from mats of single crystals prepared by slow filtration of a crystal suspension on a glass filter. The X-ray beam was directed perpendicular to the stretching direction for films and fibers, whereas it was parallel to the mat surface in the study of sedimented crystals.

Structural modeling was carried out by means of the diffraction software package of the Cerius[2] (Accelrys Inc.)[29] computer program. All calculations were run on a Silicon Graphics Octane Workstation.

Experimental Results

Structural Data. Figure 1 shows an X-ray diffraction pattern of a fiber of polyester 6 6 after being annealed under stress at 45 °C. Despite the annealing process, streaks could still be detected on the seven layer lines. A slight disorder along the chain axis direction should consequently remain, but it was still possible to measure discrete reflections on the different layer lines (Table 1). The stronger reflections are in full agreement with those previously reported by Aylwin and Boyd,[26] which define an orthorhombic unit cell. The meridional reflection indexed as 003, which suggests a slight shortening of the chain repeat from a zigzag planar conformation (≤ 0.03 nm), probably due to a distortion of the internal torsion angles, should be pointed out. 10*l* reflections are also clearly visible and define a cell with an *a* parameter of 1.008 nm. The most striking feature of the pattern is the presence of some weak reflections indexed as 01*l*, which suggests a structure defined by a unit cell with a

Table 1. Calculated and Measured Electron and X-ray Diffraction Spacings *d* (nm) for Polyester 6 6

	polyester 6 6		
index[a]	d_{calc} (nm)	d_{measd}[b,c] (nm)	d_{measd}[b,d] (nm)
220	0.415	0.415 vs E	0.415 vs
040	0.366	0.366 vs E	0.366 vs
240	0.296	0.296 s E	0.296 w
400	0.252	0.252 s E	0.252 s
420	0.238	0.238 vw E	0.238 w
260	0.220	0.220 m E	0.220 m
440	0.208	0.208 m E	0.208 w
080	0.183		0.183 w
460	0.175		0.175 vw
280	0.172		0.172 vw
620	0.164		0.164 w
640	0.153		0.153 vw
011	1.104	1.104 m off M	
101	0.865	0.865 s off M	
012	0.729	0.728 m off M	
102	0.646	0.646 s off M	
003	0.561	0.561 s M	
013	0.524	0.523 s off M	
103	0.490	0.490 s off M	
201	0.483	0.483 vw off M	
122, 202	0.484, 0.433	0.458 m off M	
104	0.388	0.388 m off M	
005	0.337	0.337 w M	
204	0.323	0.323 vw off M	
006	0.280	0.280 vw M	
226	0.232	0.232 vw off M	
027	0.228	0.228 s off M	
227	0.208	0.209 s off M	

[a] Based on an orthorhombic unit cell with $a = 1.008$ nm, $b = 1.464$ nm, and $c = 1.683$ nm. [b] Abbreviations denote relative intensities and orientations: vs, very strong; s, strong; m, medium; w, weak; vw, very weak; M, meridional; E, equatorial; off M, off meridional. [c] From X-ray fiber diffraction pattern. [d] From single-crystal electron diffraction pattern.

large value of the *b* parameter. This is doubled with respect to the previously reported one, and, consequently, the cell should contain eight molecular segments. It is worth mentioning that 10*l* and 01*l* reflections (Table 1 and Figure 1) are close enough to increase the streak appearance of the layer lines. The measured density of the fiber (1.14 g/mL) was intermediate between the calculated one for a 100% crystalline sample (1.22 g/mL) and the estimated amorphous density[26] (1.09 g/mL). A low crystallinity of 38% was deduced for the fiber sample, which was in agreement with a slightly disordered structure.

Electron diffraction patterns of single crystals (Figure 2) show *hk*0 reflections and a 2*mm* symmetry. It is worth noting that the pattern defines a rectangular unit cell with a_0 and b_0 parameters of 0.504 and 0.732 nm, respectively, which are close to the characteristic values of polyethylene and poly(alkylene dicarboxylate)s with an all-trans molecular conformation. Systematic absences for *h*00 and 0*k*0 reflections with *h* and *k* odd can be found, assuming the indicated small unit cell. Note that the large unit cells deduced from X-ray diffraction are reduced in chain axis projection to a rectangular cell containing only two chain segments. Thus, the neighboring chains along the *a* axis must have the same chain axis projection, as should also be the case of the vicinal chains along the *b* axis if a large cell with a *b* parameter of 1.464 nm is assumed.

Single-Crystal Morphology. Isothermal crystallization of polyester 6 6 in dilute *n*-octanol or *n*-hexanol solutions renders lamellar crystals whose morphology depends on the crystallization temperature, with the axial ratio being increased with

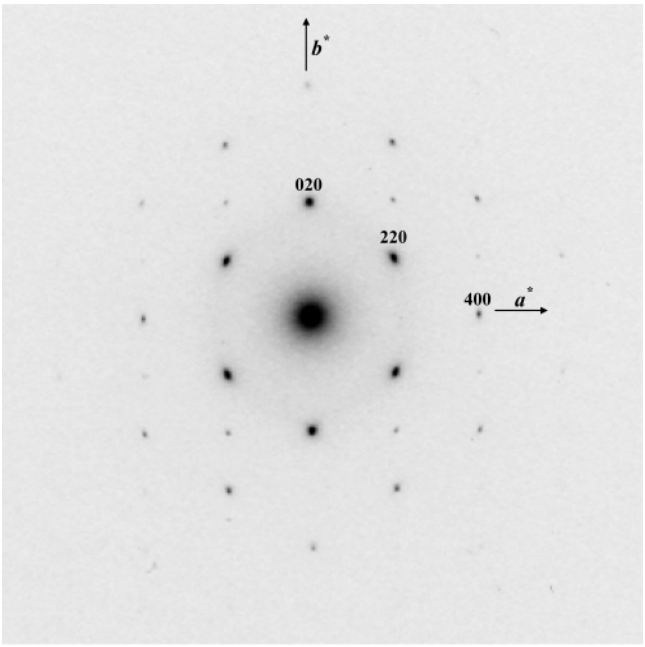

Figure 2. Electron diffraction pattern of polyester 6 6 single crystals obtained by isothermal crystallization at 0 °C in *n*-octanol. Labeled reflections are indexed according to the large orthorhombic unit cell. Note that they should be indexed as 020, 110, and 200 when the smallest unit cell is considered.

temperature (Figures 3 and 4). Similar observations have been described for polyethylene and, recently, for different polyesters.

Morphologic observations of polyester 6 6 samples deserve some additional comments. Thus, single crystals were usually obtained in crystallization from dilute *n*-octanol solutions. These corresponded to truncated lozenge crystals with lateral dimensions of several microns when the crystallization temperature was close to 0 °C (Figure 3a). Correlation of bright-field micrographs and selected area electron diffraction patterns indicates that single crystals are bounded by four {110} faces with two truncated {010} faces. The {110} growth faces form an angle of 114°, whereas a value of 123° can be measured between the {110} and {010} faces. Both angles are in agreement with those calculated from the dimensions of the planar unit cell. Crystals of polyester 6 6 become elongated along their *a* axis and show progressively more curvature on their {010} faces when the temperature is raised (Figure 3b). Thus, the l_a/l_b ratio between the lengths of the crystals along the [100] and [010] directions increased from 1.1 to 1.8 when the temperature increased from 0 to 7 °C, respectively. Crystals prepared at 7 °C show also some interesting features: a hollow with a hexagonal shape usually appears in the center of the lamellae, the {110} growth faces become slightly irregular with the appearance of some niches, and, finally, striations are frequent in the {110} sectors.

Numerous nuclei are clearly visible in low-temperature crystallizations (e.g., 0 °C). Thus, Figure 3a shows a representative lamellar crystal with nuclei placed in its center. This badly crystallized material has a round shape, although, in some cases, it seems to generate small microcrystals that appear aligned along the [100] crystallographic direction.

Multilayered crystals as well as screw dislocations of different handedness can usually be seen in the preparations carried out in *n*-hexanol (Figure 4). Crystallization at high supercooling (e.g., $T_c = 0$ °C) leads to highly irregular crystals and the above indicated nuclei, as shown in Figure 4a. It is well-known[30] that, at low temperatures, the crystallization process is controlled by

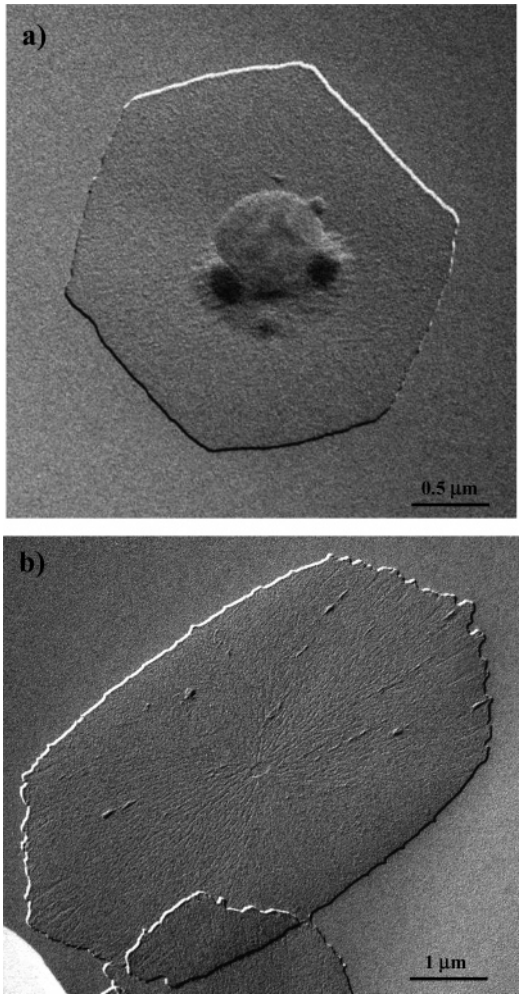

Figure 3. Electron micrographs of polyester 6 6 lamellar crystals obtained from dilute *n*-octanol solutions at 0 °C (a) and 7 °C (b). Primary nuclei are frequently observed in the center of lamellae. Crystals obtained at higher temperature show numerous striations in the {110} sectors. They are also characterized by irregular {110} and curved {010} growth faces.

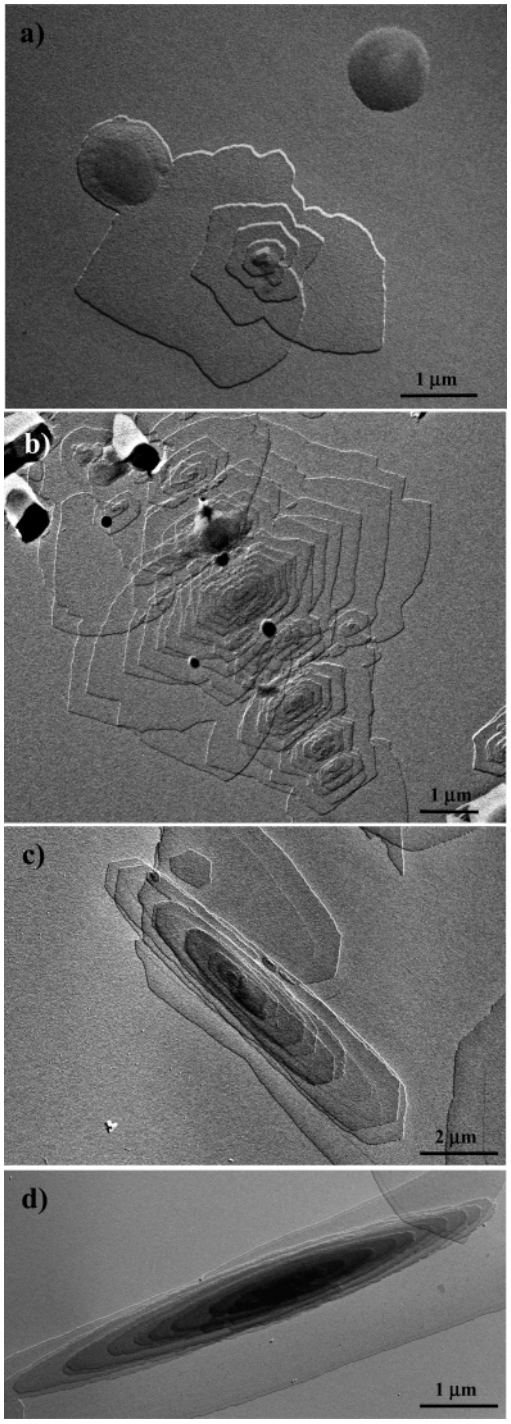

Figure 4. Electron micrographs of polyester 6 6 lamellar crystals obtained from dilute *n*-hexanol solutions at 0 °C (a), 15 °C (b), 30 °C (c), and 40 °C (d). The crystalline habit strongly depends on the crystallization temperature.

the diffusion of molecules to the growth front, which enhances the formation of dendrites. Six-sided crystals with right edges are still developed at temperatures close to 15 °C (Figure 4b). However, crystals become more extended along their [100] direction by increasing the crystallization temperature, and a lenticular morphology where the {010} face becomes rounded is attained at low supercooling (T_c = 40 °C, Figure 4d). The curved outlines of these crystals imply a rough growth surface at the molecular level, a feature extensively studied for polyethylene.[31] The l_a/l_b ratio of crystals prepared from *n*-hexanol varies from 2.6 to 5.1 or 7.9 when the temperature changes from 15 to 30 or 40 °C, respectively.

Polyester 6 6 single crystals frequently develop striations independently of the solvent used in the crystallization (e.g., Figures 3b (*n*-octanol) and 5a (*n*-hexanol)). Striations only appear in the {110} sectors and seem to be parallel oriented to the [100] crystallographic direction or with a slight deviation toward a radial direction. No perpendicular orientation to the growth faces is detected. Striations have been reported for different polyesters (i.e., polyester 4 6,[32] polyester 12 10,[18] poly-β-propiolactone,[33] and poly-ϵ-caprolactone[34]) and have merited different explanations. For example, their origin has been attributed to the existence of different chain-packing states in the crystal, a twinning involving a small chain axis shear of molecular chains, or an aggregation of microcrystals. In this way, degradation studies on poly(ϵ-caprolactone) lamellar crystals are induced to postulate a microcrystal organization.[34] Large rhombic crystals constituted by aggregates of small lathlike lamellae have also been observed in some polyamides.[35]

The crystallization studies performed with polyester 6 6 clearly show the development of lathlike microcrystals parallel to the [100] growth direction in the early stages of crystallization (Figure 3a) and even, in some cases, the development of lathlike protuberances parallel to the same direction in the {110} sectors (Figure 5b). These observations suggest a microcrystal organiza-

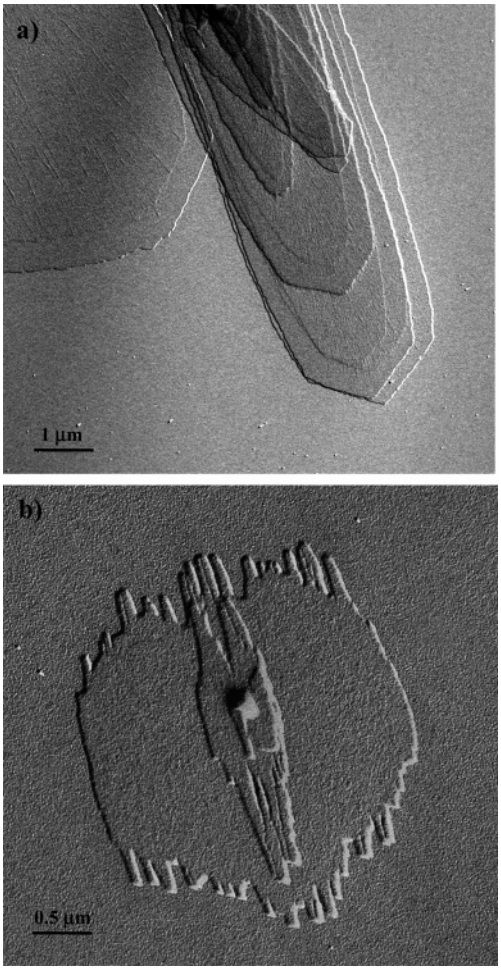

Figure 5. Electron micrographs of polyester 6 6 lamellar crystals obtained from a dilute *n*-hexanol solution at 30 °C (a) and from a dilute *n*-octanol solution at 0 °C (b). Note that microcrystals with a [100] preferential growth direction can be seen in the low-temperature crystallization, whereas striations along a practically radial direction appear in the crystals obtained at 30 °C.

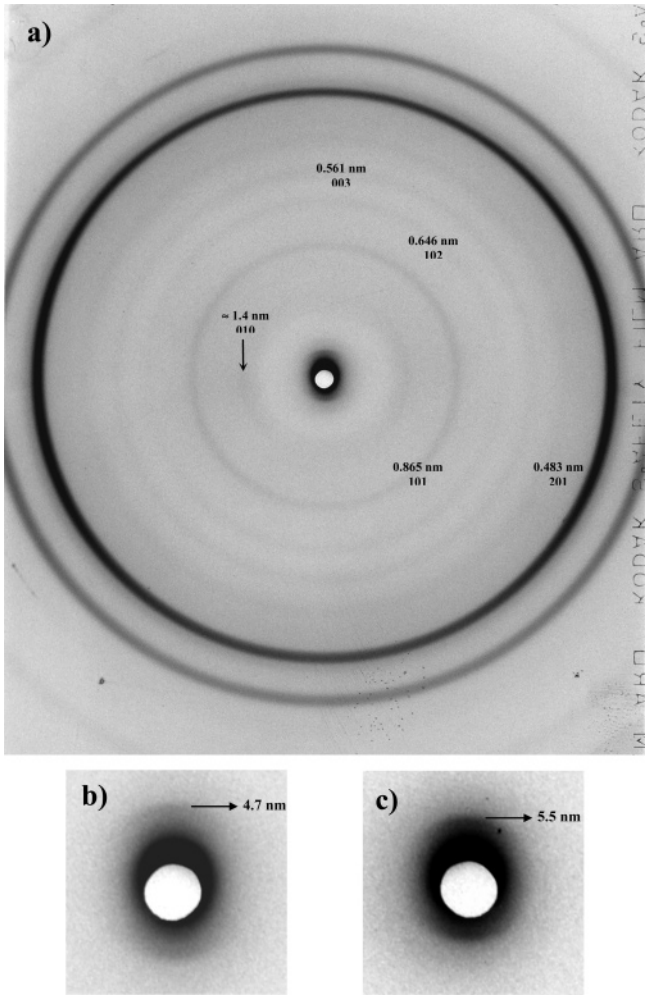

Figure 6. (a) X-ray diffraction pattern of a mat of sedimented crystals of polyester 6 6 obtained by isothermal crystallization at 30 °C in *n*-hexanol. Also shown is the second lamellar order observed in samples crystallized in *n*-hexanol at 30 °C (b) and 40 °C (c).

tion with an enhanced growth along the [100] crystallographic direction that may be the explanation for the observed striations.

The electron diffraction patterns demonstrate that molecular chains are perpendicular oriented to the crystal basal plane and allow a lamellar folding to be inferred when the high molecular weight of the polymers and the reduced lamellar thickness are also taken into account.

Diffraction patterns of the mats of the sedimented crystals show low angle reflections associated to different lamellar orders and wide angle reflections that are fully compatible with those observed in the X-ray fiber diffraction patterns (Figure 6). A single structure is consequently found in fibers processed from the melt and in the solution-grown single crystals. The main difference corresponds to the absence of 01*l* reflections in the mat patterns, which may be due to their low intensity or to a more regular packing where the *b* axis is not doubled. However, the diffuse ring observed at a spacing slightly greater than 1.4 nm must be pointed out. Patterns obtained from samples crystallized at different temperatures only differ in the low angle reflections associated with a regular stacking of lamellae. An increase of the spacing with temperature was detected. Thus, crystals obtained from *n*-hexanol at 30 °C had a lamellar thickness close to 9.4 nm (Figure 6), whereas, when the temperature was raised to 40 °C, the thickness increased to 11.0 nm. Values close to 10 nm were estimated from the shadows of the crystals in the electron micrographs.

Polyethylene decoration highlighted the sectorization of the single crystals and also supported a regular folding mechanism (Figure 7a). The decorating rods were preferentially placed perpendicular to the {110} and {010} growth faces, thus suggesting that the chain folding is parallel to the indicated planes. In fact, folds may take place between neighboring chains along both the [220] and the [100] directions since molecular chains are adirectional. This feature is not feasible in some directional polyesters such as hydroxyacid derivatives since an antiparallel molecular chain arrangement is only established along the [110] diagonal directions of their unit cells.[36] These observations are consistent with the characteristic polymer crystal growth that occurs normal to the fold planes, which stack successively on top of each other as they are nucleated and filled out with folded chains.

Enzymatic Degradation of Lamellar Crystals. Figures 7b and 8 show the electron micrographs of polyester 6 6 lamellar crystals obtained under different crystallization conditions and after partial degradation by an enzyme with a moderate activity such as the lipase from *Pseudomonas cepacia*. These Figures illustrate how hydrolysis by enzymatic attack mainly progressed from the {110} crystal faces, thus giving rise to highly irregular borders with a fringed texture that develops parallel to the [100] crystal direction. This feature suggests the existence of stronger

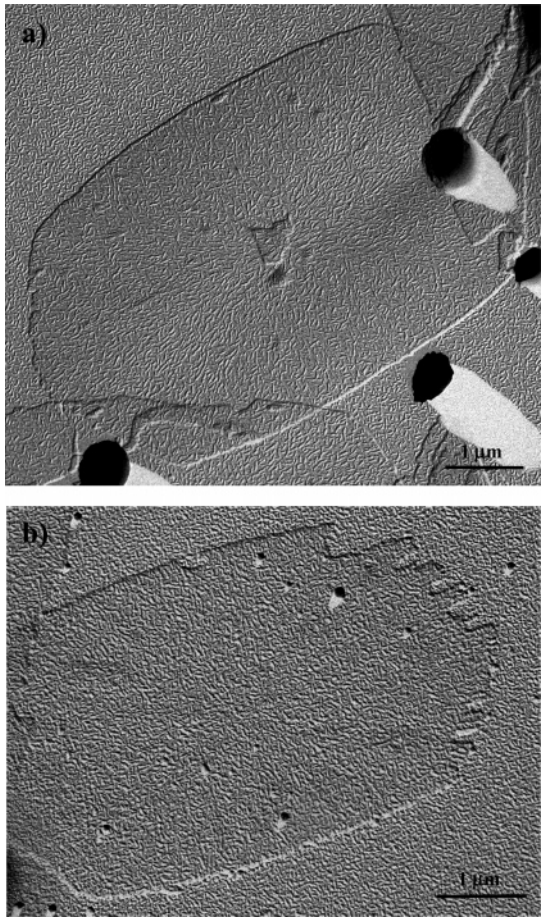

Figure 7. Polyethylene decoration of polyester 6 6 lamellar crystals obtained from *n*-octanol at 10 °C before (a) and after (b) exposure to a lipase (*Pseudomonas cepacia*) medium at 37 °C for 45 min.

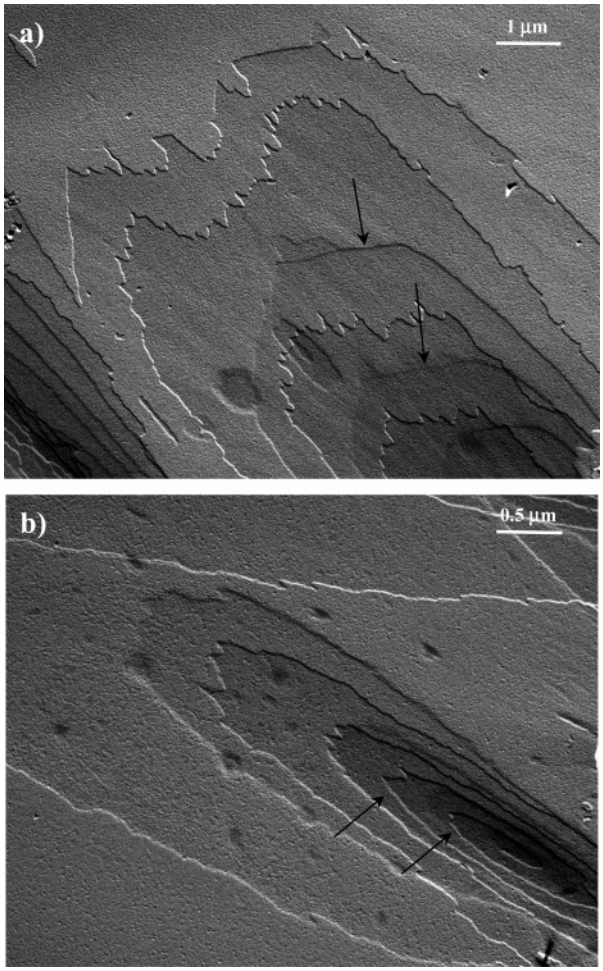

Figure 8. Electron micrographs of polyester 6 6 lamellar crystals obtained from dilute *n*-hexanol solutions at 30 °C (a) and 40 °C (b) and exposed to a lipase (*Pseudomonas cepacia*) medium at 37 °C for 45 min. Arrows indicate lamellae not exposed to enzymatic attack (a) and lenticular crystals with regular edges (b).

packing interactions along the indicated direction and may justify the presence of the observed striations as a consequence of the assembly of microcrystals with a preferred [100] growing direction. It should be pointed out that straight edges are clearly visible (see arrows) in the lamellae that are deposited under the other ones, and are consequently not exposed to enzymatic attack. Thus, the irregularities observed on the upper lamellae are only a consequence of the hydrolysis process. Degradation is slower in the curved {010} faces, as can be clearly observed when crystals with a lenticular morphology are exposed to degradation. Figure 8b shows how the crystals without {110} faces (see arrows) are practically unaltered despite being the upper lamellae of the multilayered growth.

Lamellar thickness before and after exposure remains practically constant providing no evidence of enzymatic degradation on the lamellar surface. Furthermore, GPC analysis showed that the molecular weight of crystals remained unchanged before and after the enzymatic attack with the lipase from *Pseudomonas cepacia*. In this way, elution curves have the same shape and show similar average values (i.e., $M_w = 25\,500$ g/mol and $M_n = 14\,400$ g/mol before exposure, and $M_w = 25\,200$ g/mol and $M_n = 13\,500$ g/mol after 45 min of exposure). No partial degradation seems to take place at the folding surface. Similar observations have recently been reported for the degradation study of poly(ethylene succinate)[16] lamellar crystals. Three reasons were given for the absence of the surface degradation: (a) a steric hindrance on the lamellar surface to the active site of the enzyme, (b) the absence of labile ester groups in the chain folding, and (c) a degradation rate of the exo-type activity of the enzyme that is faster than that of the endo-type.

Polyethylene decoration of the exposed single crystals (Figure 7b) shows that the lamellar surface became highly disordered, contrasting with the regular surface observed before exposure (Figure 7a). In this way, enzymes may interact with the folding surface, although the attack seems to proceed at a very slow rate.

Figure 9 shows the electron micrograph of crystals exposed to a lipase from *Rhizopus arrhizus*, which has a greater enzymatic activity than the lipase previously used. In this case, all crystal faces appear highly irregular, and, furthermore, great holes are clearly visible on the surface of the lamellar crystals (see asterisks). Again crystals covered by other lamellae show a regular morphology (see arrows), demonstrating that irregularities are only a consequence of the enzymatic attack. It seems that steric impediments cannot completely prevent the attack of this lipase and that some ester groups may exist on the lamellar surface. These may correspond to loose loops that are first hydrolyzed by the enzyme molecules and then removed from the crystals. As explained before for poly(ethylene succinate),[15] a hole can thus be originated, and then the enzyme could enlarge the hole by attacking its edge sides. Note that lamellar thickness is unaffected since the shadows of the hole walls and the faces of the nondegraded crystals are similar (Figure 9).

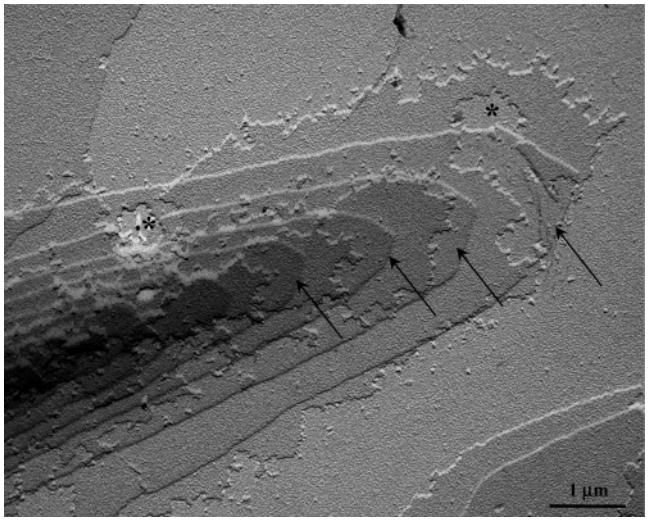

Figure 9. Electron micrograph of polyester 6 6 lamellar crystals obtained from dilute *n*-hexanol solutions at 30 °C and exposed to a lipase (*Rhizopus arrhizus*) medium at 37 °C for 30 min. Arrows indicate lamellae not exposed to enzymatic attack, whereas holes are labeled with asterisks.

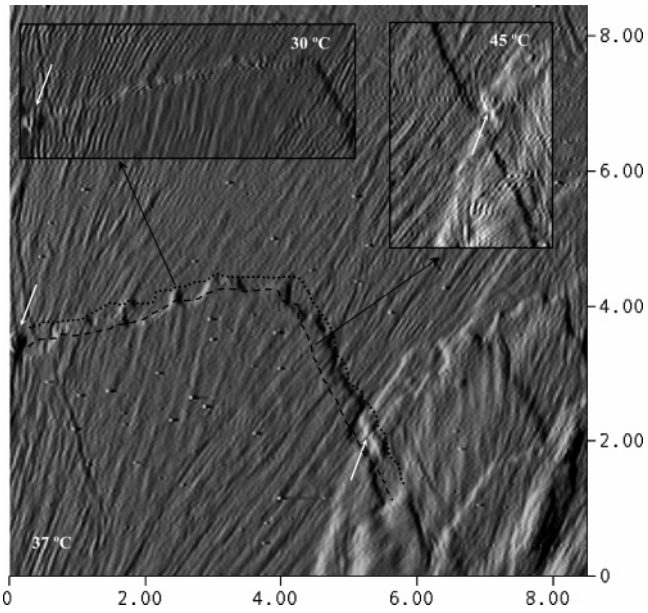

Figure 10. AFM phase images of a polyester 6 6 lamellar crystal obtained from a dilute *n*-hexanol solution at 30 °C and taken at the indicated temperatures of 30, 37, and 45 °C after 10 min of storage. Dashed and dotted lines indicate the lamellar edges at 45 and 30 °C, respectively. White arrows indicate reference points that are useful to compare the lamellar edges in the different micrographs. Scale axes are in micrometers.

The effects of temperature on the lamellar morphology of polyester 6 6 have also been studied by using a temperature-controlled AFM equipped with a heating stage since degradation experiments were performed at 37 °C, which is a temperature close to the melting point of crystals. Minor changes were detected on the lamellar borders between 30 and 45 °C, with a slight contraction of the lamellar edges being observed when the temperature increased (Figure 10). However, changes were not significant compared with those observed after exposure to the enzymatic medium.

The AFM height image and line profile data of the multilayered lamellar crystals obtained at 30 °C indicates a fairly constant monolamellar thickness close to 10.0 nm, in agreement with X-ray diffraction data of mats of sedimented crystals. An increase in temperature (from 30 to 40 °C) did not cause a significant change in the average crystal thickness, although a rougher lamellar surface was detected.

Molecular Simulation. Molecular simulation was tentatively carried out assuming a practically all-trans molecular conformation due to the small shortening deduced from the X-ray diffraction patterns. This conformation is compatible with a 2/*m* molecular symmetry with inversion centers in the middle of both the diol and the dicarboxylic units, with the mirror plane and the binary axis symmetry being lost when torsional angles deviate from 180°.

The setting angle of the molecular chains was refined taking into account the experimental intensities of the *hk*0 electron diffraction patterns. Furthermore, simulation was facilitated by considering that the chain axis projection of the structure could be well defined by a small rectangular unit cell ($a = 0.504$ nm, $b = 0.732$ nm) containing only two molecular segments (Figure 11b). Systematic absences (*h*00 and 0*k*0 with *k* and *h* odd) were detected for this small cell, indicating that both segments could be related by a glide plane parallel to the *a* or the *b* crystallographic axis.

The rotation angle around the fiber axis, defined as τ in Figure 11b, and the temperature factor were the variables considered at this stage. The angle was varied in small intervals of 1° from 0 to 90°. The best fit corresponded to an *R* factor of 0.09 that was attained with a τ angle of 46°. A variation of ±14° for the setting angle yielded a value larger than 0.15 for this figure of merit. No improvement was obtained by considering isotropic thermal factors. Table 2 shows the observed and calculated structure factors, whereas Figure 12 displays the electron diffraction pattern simulated with the Cerius[2] program for the optimized conditions. We have also modified the molecular conformation to exactly fit the experimental chain axis repeat. This feature was achieved varying only the $CH_2CH_2-OC(O)$ and $OC(O)-CH_2CH_2$ torsion angles to a value of ±135°. However, the simulation of the electron diffraction pattern was always noticeably worse, with an *R* factor of 0.19 being the best figure. This result suggests that all torsion angles may be slightly deviated from 180°, as has been reported for the structure of polycaprolactone solved by direct methods.[37]

In a second stage, we simulated the X-ray fiber diffraction pattern considering an orthorhombic unit cell containing four chain segments ($a = 1.008$ nm, $b = 0.732$ nm, and $c = 1.683$ nm). Thus, we ignored the weak signals that suggest a double value of the *b* parameter. A $Pb2_1a$ space-group symmetry was considered (Figure 11a) since it appeared to be the most suitable. Note, for example, that neighboring chains along the *a* axis must be identical in chain axis projection, justifying the small cell defined in the first modeling step. A glide plane relates molecular segments 1 and 2, as explained before, and the systematic absence rule can be fulfilled. Segment 1 was progressively shifted along the *c* chain axis direction to qualitatively fit the experimental X-ray fiber diffraction pattern to that simulated by the Cerius[2] program, whereas the setting angle was maintained at 46 or 226°. The *z* fractional coordinate of a representative oxygen atom of a diol unit was used to define the axial shift of molecule 1, with the position of the remaining chains being fixed by the space-group symmetry. The best agreement was obtained when this fractional coordinate was 0.08. The corresponding simulated pattern is shown in Figure 13a. The weaknesses of the fifth layer line and the 003 reflection that contrast with the experimental observations are worth noting.

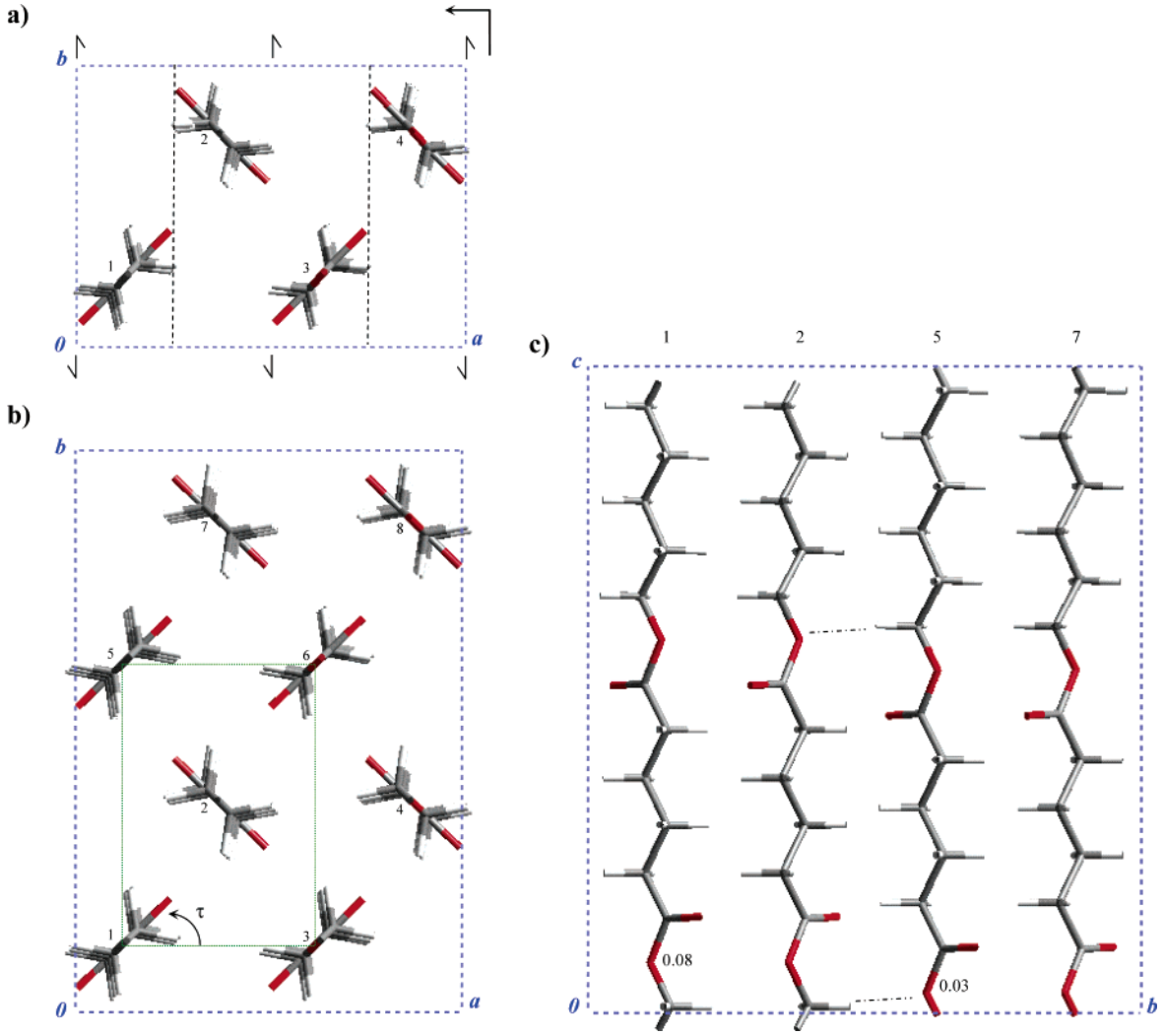

Figure 11. (a) View parallel to the *c*-axis direction showing the packing of polyester 6 6 assuming a reduced unit cell with a $Pb2_1a$ space group. Symmetry elements are indicated, and molecules are labeled according to the explanation given in the text. (b) View parallel to the *c*-axis direction showing the packing of polyester 6 6 assuming a large unit cell with a *b* parameter of 1.464 nm. In projection, this packing can be defined by the smaller rectangular cell containing two chain segments (green dashed lines), whose orientation is defined by the τ setting angle. (c) View along the *a*-axis direction of the proposed structure of polyester 6 6. The axial position of molecular chains 1 and 5 is indicated by the *z* fractional coordinate of an oxygen atom. Dashed and dotted lines indicate the alignment between the closer CH_2 groups and O atoms of chains 2 and 5. Color code: white = hydrogen; gray = carbon; red = oxygen.

Table 2. Observed (F_0) and Calculated (F_c) Electron Beam Structure Factors for Polyester 6 6

			d(obs)			F_c ($\tau = 32°$)	F_c ($\tau = 40°$)	F_c ($\tau = 46°$)			F_c ($\tau = 52°$)	F_c ($\tau = 60°$)
h	*k*	*l*	(nm)	m^a	$F_0{}^b$	$B^c = 0$	$B^c = 0$	$B^c = 0$	$B^c = 5$	$B^c = 10$	$B^c = 0$	$B^c = 0$
2	2	0	0.415	2	101.73	106.46	103.84	101.73	94.61	87.99	99.61	96.95
0	4	0	0.366	1	92.78	73.99	82.07	88.45	80.57	73.39	94.82	102.87
4	0	0	0.252	1	57.81	61.51	53.54	47.30	38.85	31.90	40.94	32.64
2	6	0	0.220	2	37.42	29.01	33.87	38.17	29.46	22.73	42.67	48.10
4	4	0	0.208	2	37.02	39.69	36.28	33.41	24.99	18.70	30.73	28.13
2	4	0	0.296	2	34.26	28.63	31.60	32.18	27.91	24.20	31.28	27.83
0	8	0	0.183	1	33.19	21.75	28.88	33.09	22.78	15.68	36.20	39.50
6	2	0	0.164	2	25.28	33.76	29.15	25.61	16.07	10.08	21.96	16.75
4	2	0	0.238	2	22.42	16.64	17.92	18.33	14.71	11.80	18.21	16.99
2	8	0	0.172	2	14.91	15.12	13.64	11.99	7.86	5.15	10.55	9.31
6	4	0	0.153	2	11.84	12.27	13.79	14.67	8.58	5.02	15.66	16.61
4	6	0	0.175	2	11.76	20.35	23.77	24.47	16.29	10.85	23.26	19.19
						$R^d = 0.15$	$R^d = 0.11$	$R^d = 0.09$	$R^d = 0.17$	$R^d = 0.24$	$R^d = 0.14$	$R^d = 0.21$

[a] Multiplicity. [b] All equivalent spots have a similar intensity. [c] Temperature factor in Å^2. [d] *R* factor calculated as $\sum m \cdot |F_0 - F_c| / \sum m \cdot F_0$. In each case, the F_0 was escalated to minimize the difference between calculated and observed structure factors.

In the third refinement stage, we enlarged the cell to the final dimensions by considering a slight chain axis shift between neighboring chains along the *b* axis. The structure was consequently defined by a *P11a* space group of lower symmetry and an asymmetric structural unit constituted by four molecular segments (1, 2, 5, and 7 in Figure 11b). However, the former

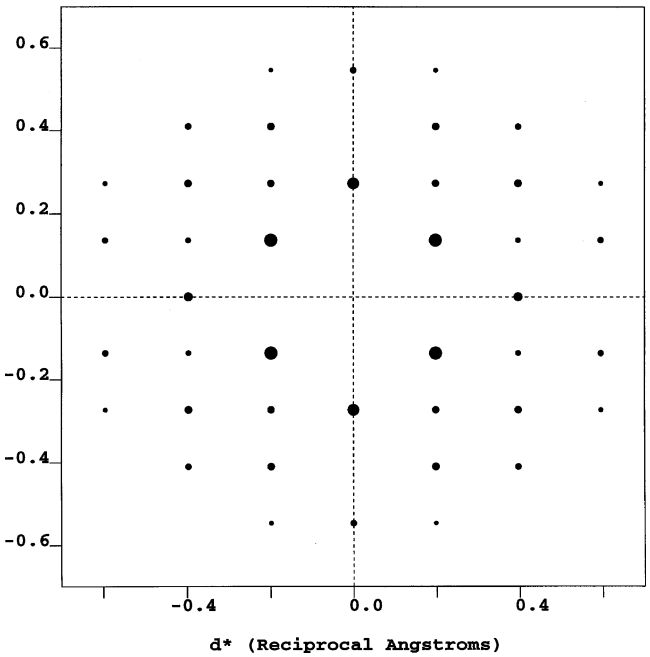

Figure 12. Simulated *hk*0 electron diffraction pattern of the refined structure of polyester 6 6 ($\tau = 46°$).

symmetry relationship between segments 1 and 2 was maintained and was also applied to segments 5 and 7. The molecular segment 5 was slightly shifted to give rise to the low intensity 01*l* reflections detected in the experimental X-ray fiber patterns. Furthermore, the intensities of the fifth layer line and indeed of the 003 reflection could be similar to those of the experimental observations. The best pattern (Figure 13b) was obtained with a shift of 0.05 between molecules 1 and 5 (Figure 11c), which allows interactions between the **CH**$_2$−O methylene groups and the CH$_2$-**O** oxygen atom of the diol unit to be established. These units correspond to the most electrostatically positive groups and the most electrostatically negative atoms, respectively.

Conclusions

The results reported in this work, together with those previously published, indicate that aliphatic polyesters with a high methylene content in their repeat unit have a rather complex molecular packing despite their similarities with polyethylene. However, the chain axis projection of these structures can be well defined by a rectangular unit cell with a similar dimension to polyethylene and by an orientation of molecular segments that is also similar to that found in polyethylene (setting angles close to ±45°). The improvement of electrostatic interactions might be the main reason for these two main observations: (a) the molecular conformation was slightly deviated from a planar zigzag conformation, and (b) the packing was characterized by a large unit cell where neighboring chains along the *a* or *b* crystallographic axes could have a nonprogressive shift along the chain axis direction.

Single crystals with six lateral sides (four {110} and two {010} faces) were the basic structures found for polyester 6 6, with their aspect ratio being highly influenced by the crystallization temperature. Curved crystals with a predominant growth along the [100] direction were favored at high crystallization temperatures. Striations with an orientation radial or practically parallel to the [100] direction were detected in the {110} sectors, and these irregularities were enhanced by the influence of temperature. Badly crystallized samples showed niches and

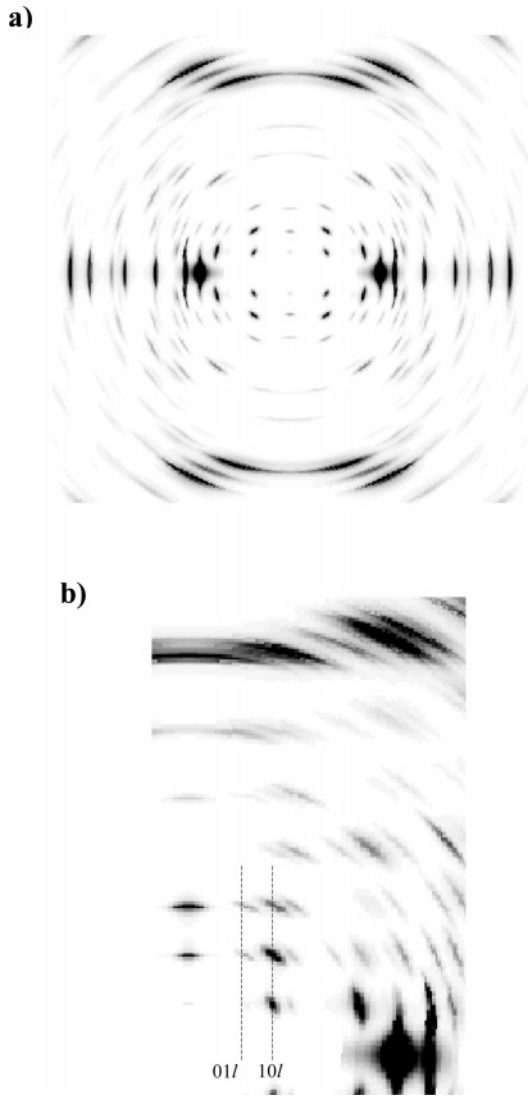

Figure 13. (a) Simulated X-ray fiber diffraction pattern of the optimized structure assuming the small unit cell with a *Pb2*$_1$*a* symmetry. (b) Simulated X-ray fiber diffraction pattern of the refined structure of polyester 6 6 assuming a large unit cell with a *b* parameter of 1.464 nm. The pattern corresponds to a fiber tilt of 10° to enhance the 003 reflection. Only a quadrant has been drawn to clearly show the 01*l* reflections.

sometimes microcrystals, both cases with the fastest growth direction along [100]. Decoration techniques demonstrate that the surface of lamellar crystals was ordered and that the folding was parallel to the crystal edges in the different sectors.

Enzymatic degradation of single crystals with lipases of moderate activity progressed from the crystal edges rather than from the chain-folding surfaces. Lamellar thickness remained practically constant during the enzymatic attack, but decoration revealed that some minor changes took place on the folding surface. Degradation mainly progressed from the {110} faces, giving rise to a fringed texture that may be related to a microcrystal organization and may justify the presence of the observed striations.

Acknowledgment. This research has been supported by the CICYT and FEDER (Grant MAT 2003-01004). We would like to express our gratitude to Jordi Díaz of the Scientific-Technical Services of UB for the AFM micrographs.

CDV

References and Notes

(1) Ginde, R. M.; Gupta, R. K. *J. Appl. Polym. Sci.* **1987**, *33*, 2411.
(2) Vert, M.; Li, S.; Garreau, H. *Clin. Mater.* **1992**, *10*, 3.
(3) Chu, C. *Wound Closure Biomaterials and Devices*; CRC Press: Boca Raton, FL, 1997; Chapter 5, pp 65−106.
(4) Pack, J. W.; Kim, S. H.; Cho, I. W.; Park, S. Y.; Kim, Y. H. *J. Polym. Sci., Polym. Chem. Ed.* **2002**, *40*, 544.
(5) Dawes, E. A.; Senior, P. J. *Adv. Microb. Physiol.* **1973**, *10*, 135.
(6) Anderson, A. J.; Dawes, E. A. *Microbiol. Rev.* **1990**, *54*, 450.
(7) Holmes, P. A. *Developments in Crystalline Polymers*; Basset, D. C., Ed.; Elsevier Applied Science: New York, 1988; Vol. 2, pp 1−65.
(8) Machizuki, M.; Hirami, M. *Polym. Adv. Technol.* **1996**, *8*, 203.
(9) Batzer, H. *Makromol. Chem.* **1951**, *5*, 5.
(10) Takiyama, E.; Fujimaki, T. *Biodegradable Plastics and Polymers;* Doi, Y., Fukuda, K., Eds.; Elsevier Science: New York, 1994; p 150.
(11) Murase, T.; Iwata, T.; Doi, Y. *Macromolecules* **2001**, *34*, 5848.
(12) Iwata, T.; Shiromo, M.; Doi, Y. *Macromol. Chem. Phys.* **2002**, *203*, 1309.
(13) Marchessault, R. H.; Kawada, J. *Macromolecules* **2004**, *37*, 7418.
(14) Kikkawa, Y.; Abe, H.; Iwata, T.; Inoue, Y.; Doi, Y. *Biomacromolecules* **2002**, *3*, 350.
(15) Gan, Z.; Abe, H.; Doi, Y. *Biomacromolecules* **2000**, *1*, 713.
(16) Iwata, T.; Doi, Y.; Isono, K.; Yoshida, Y. *Macromolecules* **2001**, *34*, 7343.
(17) Fuller, C. S. *J. Am. Chem. Soc.* **1939**, *61*, 2575.
(18) Kanamoto, T.; Tanaka, K. *J. Polym. Sci., Part A-2* **1971**, *9*, 2043.
(19) Ueda, A. S.; Chatani, Y.; Tadokoro, H. *Polym. J.* **1991**, *2*, 387.
(20) Aylwin, P. A.; Boyd, R. H. *Polymer* **1984**, *25*, 323.
(21) Liau, W. B.; Boyd, R. H. *Macromolecules* **1990**, *23*, 1531.
(22) Brandrup, J.; Immergut, H. *Polymer Handbook*; Wiley: New York, 1989; Chapter VI.
(23) Almontassir, A.; Gestí, S.; Franco, L.; Puiggalí, J. *Macromolecules* **2004**, *37*, 5300.
(24) Gestí, S.; Almontassir, A.; Casas, M. T.; Puiggalí, J. *Polymer* **2004**, *45*, 8845.
(25) Minke, R.; Blackwell, J. *J. Macromol. Sci., Phys.* **1979**, *B16*, 407.
(26) Aylwin, P. A.; Boyd, R. H. *Polymer* **1984**, *25*, 323.
(27) Wittmann, J. C.; Lotz, B. *J. Polym. Sci., Part B: Polym. Phys.* **1985**, *23*, 205.
(28) *ELD*$^{2.1}$*: Quantitative Electron Diffraction*; Calidris: Sollentuna, Sweden, 2001.
(29) *Cerius*^{2}; Accelrys Software Inc.: Cambridge, UK, 2001.
(30) Bassett, D. C.; Keller, A. *Philos. Mag.* **1962**, *7*, 1553.
(31) Toda, A. *Crystallization of Polymers*; Dosiere, M., Ed.; Kluwer Academic Publishers: Dordrecht/Boston/London, 1993; pp 141−152.
(32) Pouget, E.; Almontassir, A.; Casas, M. T.; Puiggalí J. *Macromolecules* **2003**, *36*, 698.
(33) Furuhashi, Y.; Iwata, T.; Sikorski, P.; Atkins, E.; Doi, Y. *Macromolecules* **2000**, *33*, 9423.
(34) Iwata, T.; Doi, Y. *Polym. Int.* **2002**, *51*, 852.
(35) Navarro, E.; Alemán, C.; Subirana, J. A.; Puiggalí, J. *Macromolecules* **1996**, *29*, 5406.
(36) Hocking, P. J.; Marchessault, R. H.; Timmins, M. R.; Lenz, R. W.; Fuller, R. C. *Macromolecules* **1996**, *29*, 8330.
(37) Hu, H.; Dorset, D. L. *Macromolecules* **1990**, *23*, 4604.

BM050860D